Some unsteady propulsive characteristics of a podded propeller unit under maneuvering operation

Liu, Pengfei; Islam, Mohammed; Veitch, Brian

Publisher's version / Version de l'éditeur:

Proceedings of the First International Symposium on Marine Propulsors - smp'09, pp. 507-516, 2009-01-01

National Research Council Canada
Conseil national de recherches Canada

Institute for Ocean Technology
Institut des technologies océaniques

IR-2009-07

Institute Report

Some unsteady propulsive characteristics of a podded propeller unit under maneuvering operation.

Liu, P.; Islam, M.; Veitch, B.,

Liu, P.; Islam, M.; Veitch, B., 2009. Some unsteady propulsive characteristics of a podded propeller unit under maneuvering operation. 1st International Symposium on Marine Propulsors, 22-24 June 2009, Trondheim, Norway WA4-4 : 10 p.

First International Symposium on Marine Propulsors
Smp'09, Trondheim, Norway, June 2009

Some Unsteady Propulsive Characteristics of a Podded Propeller Unit under Maneuvering Operation

Pengfei Liu[1], Mohammed Islam[2] and Brian Veitch[3]

[1]National Research Council Canada, Institute for Ocean Technology, St. John's, NL Canada
[2]Oceanic Consulting Corporation, St. John's, NL Canada
[3]Faculty of Engineering & Applied Science, Memorial University of Newfoundland, St. John's, NL Canada

ABSTRACT

Propulsion dynamics of a podded propulsor unit in steering motion at fixed azimuth angles were investigated numerically. Unsteady forces, torques and bending moments were predicted for a model podded propulsor unit at various azimuth angles. Analysis was performed for averaged forces and their fluctuations as well. A time-domain unsteady multi-body panel method code, PROPELLA, was further developed for this work. Predictions were compared with a set of time averaged in-house experimental data for a puller type podded propulsor configuration in the first quadrant operation. Unsteady fluctuations of forces were predicted numerically. Analysis was made for the bending moment on propeller blades, shaft and the propulsor unit stock shaft for azimuth angles from 0 to 45 degrees. It indicates that the magnitude and fluctuation of the forces are significant and they are essential for structural strength and design optimization. The predicted bending moment and global forces on the propulsor unit provide some useful data for ship maneuvering motion and simulation at off design conditions.

Keywords
Podded propulsor; Propulsor Simulator; Propeller unsteady loads; Panel Methods

1 INTRODUCTION

Research and development on propulsion hydrodynamics prediction, design optimization and performance evaluation for traditional marine propellers are extensive in the literature. Among these, the first attempt of using panel method for a propeller was made in the mid 1980's (Hess and Valarezo 1985), and examples of panel method application to marine propellers include the work by Kerwin and others (Kerwin et al. 1987) and some work at Mitsubishi (Hoshino 1993) to name a two. However, R&D activities for the podded propulsor units became noticeable only since around 2000. With a dramatic increase in application and installation of podded propulsors, structural and bearing failures became prevalent and hydrodynamic design optimization became important. Therefore, systematic research and development work, both experimentally and numerically became necessary. Prior to mid 2000's, R&D work on podded propulsors was mostly performed by individual shipbuilders internally. Published results were rare. To address these issues, a collaborative R&D program was initialized in 2001 among Memorial University of Newfoundland (MUN), Institute for Ocean Technology (IOT) of National Research Council Canada (NRC), Oceanic Consulting Corporation and Thordon Bearing Ltd.

The podded propeller research program contains both experimental and numerical components. The goal of the numerical work is to develop a robust and reliable numerical tool with a suite of capabilities to perform tasks such as propulsive characteristics and unsteady structural load prediction, and performance evaluation and design optimization of podded propeller units. In the past seven years, a propeller panel method code, PROPELLA, was adopted and used as the main prediction tool to address the needs for podded propulsor simulations. Numerical tools need verification and validation before they can be used but verification and validation with a good agreement with analytical and experimental measurements are not the ultimate goal of a numerical work. This numerical tool, in addition to being able to produce the same kind of results as from experimental measurements in a cost effective and timely fashion, was used to produce important results that are impossible or difficult to obtain from experimental measurements. These results include unsteady propeller blade spindle torque, in-plane and out-of-plane bending moments about arbitrary axes, and the propulsor unit's transient global force and moments with respect to any arbitrary axes.

The hydrodynamics kernel of the code is a classical panel method. It is a low order time-domain panel method formulated similar to many other panel methods, such as PMARC developed at NASA Ames Research Centre (Katz and Plotkin 1991). The backbone of the current panel method code was initially developed to simulate marine swimmers with lunate tails (Liu 1996a, Liu & Bose 1997, and Liu & Bose 1999). The code PROPELLA was then developed for an ice-class propeller research program (Liu 1996b and Veitch et al. 1997). Inflow wake and hyperboloid panel algorithm were studied and implemented as well (Liu & Bose 1998), followed by a semi-empirical cavitation model to predict propeller cavitation performance (Liu et al. 2001a). In the meantime, automated surface mesh generation of arbitrary configuration for a propeller to interact with rudder, nozzle, ice blockage etc. along with induced velocity downstream and wake roll-up were implemented (Liu et al. 2001b). A 3D unsteady data visualization scheme using MFC (C++) and OpenGL was implemented as well (Liu 2002). A more robust and reliable iterative pressure Kutta using Broyden's method, rather than the traditional Newton Raphson method, was developed in 2002 (Liu et al. 2002). Podded propeller geometry was implemented and a comparative study between puller and pusher type podded propulsors was performed (Islam 2003 and Islam et al. 2006). A shed vortex impingement algorithm was developed recently (He et al. 2007a and 2007b) and was validated via an in-house experimental research program (He 2005 et al.). A multiple-body panel method formulation was developed and used for wind-in-ground thruster simulation about the same time (Liu 2005). A propeller design and optimization procedure was developed and was applied to a Canadian Coast Guard ice breaker, a dual-tunnel shallow hull Eckaloo (Liu et al. 2006). This multiple-body multiple-path panel method was extended for propeller and ice interaction recently (Liu et al. 2008).

Time averaged blade and pod unit stock force of a podded propulsor at an azimuth angle during maneuvering for pusher and puller configurations were obtained in-house via experimental measurements only recently (Islam et al. to be submitted). These, to the authors' knowledge, are the first set of results available in open literature. These time average forces give an indication of the structural loading of the podded propeller units and its components and are essential for numerical code validation. The main purpose of the current work is to obtain unsteady force fluctuation for structural strength evaluation and design consideration in terms of bearings and shaft/stock fatigue failure and structural strength analysis. The predicted forces and torques/moments and their fluctuations are also the basic data for the estimate of ship motion during maneuvering. In the following sections, we will briefly discuss code implementation, and validation against the time averaged forces of a podded propeller unit and its shaft components. Predictions of both time averaged and real-time fluctuations of the forces, torques and moments on the shaft and stock of the podded propeller units were then shown and analyzed.

2 NUMERICAL METHOD AND IMPLEMENTATION NOTE

As mentioned earlier, the hydrodynamic kernel of the code is a low-order, potential follow based time-domain panel method. An introduction to the method was discussed systematically by Katz and Plotkin (1991). A detailed formulation of this boundary element method in a general and in multiple-object and multiple-path format was presented in (Liu 1996a) and (Liu & Bose 1997), respectively. A detailed algorithm implementation of the multiple-object, multiple path panel method to simulate interaction between propeller and other objects was given for an ice-class propeller approaching and interacting with an ice blockage (Liu et al. 2008).

The code was implemented by assuming that multiple objects are moving in their different paths in an acquiescent fluid. At each time step, the body-frame of the podded propeller moves forward with a distance δd, and rotates about its shaft centre with $\delta\alpha$. At the same time step, the translated and rotated propeller body frame is further rotated about a transversal axis passing through the origin of the body frame with a constant angle of β to obtain a desired shaft inclination angle (the trim angle $\beta=0$ for the podded propeller in this study). The final rotation about the centerline of the stock of the podded propeller unit is then made, with a constant value of θ to simulate a fixed azimuth angle during maneuvering. Figure 1 shows the coordinate system of the propeller body-frame of the propeller-pod-strut assembly and the global (inertia) frame.

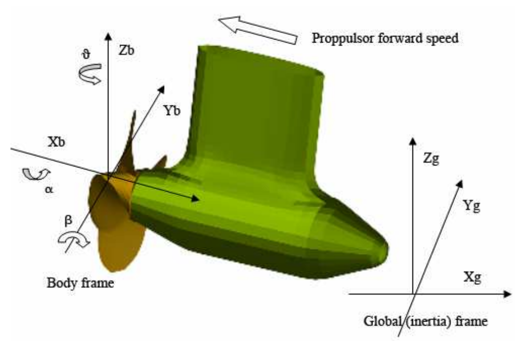

Figure 1. Propeller body-frame coordinates system along with its pod and strut geometry.

The code was developed to handle multiple-object and multiple-path motion. When propeller, pod and strut are all meshed properly and move forward at the same velocity, it simulates a podded propulsor in operation.

Figures 2A and 2B show the torque and moments on propeller shaft and stock of the propulsor units.

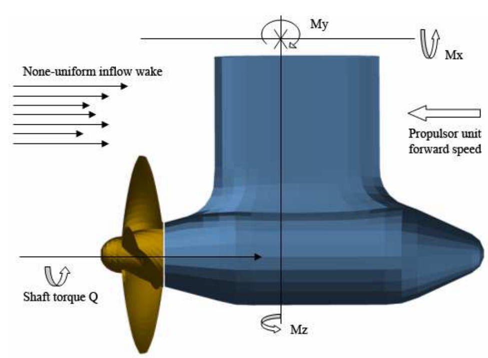

Figure 2A.Torque and moment definition side view.

In figure 2A, variable Q is propeller shaft torque about the centerline of the shaft. Variable M_z is the spindle torque (coefficient in data plots) about the stock centre of the propulsor unit and M_y and M_x are the in-plane and out-of-plane bending moments (coefficients in data plots) at the root of the strut. The code can also take prescribed inflow wake to simulate incoming flow field located at the propeller disk plane astern.

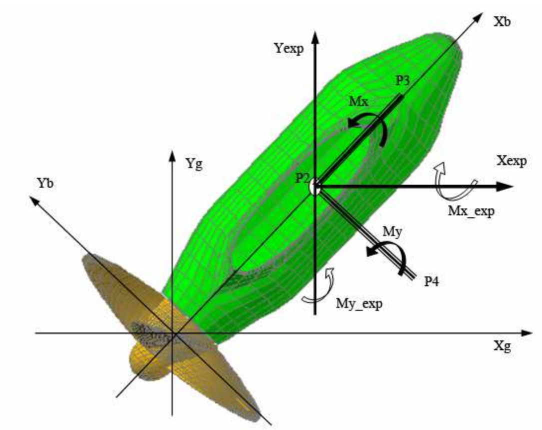

Figure 2B. Stock moment vector definition top view.

Figure 2B shows the top view of the stock spindle torque and bending moment definitions and comparison of the moment vector orientation between the code and the experimental set up. In PROPELLA (Liu 1996-2009), the origin of the propeller-pod-strut assembly is defined at the origin of the propeller. As shown in figure 2B, the body frame is denoted by *(X_b, Y_b, Z_b)* and the inertial frame by *(X_g, Y_g, Z_g)*. The bending moment vectors of M_x and M_y in PROPELLA are based on the body frame, as shown in figure 2B as lines P_2-P_3 and P_4-P_2, respectively. In the experimental set-up, propulsor unit's stock bending moments were defined differently, which are parallel and perpendicular to the longitudinal line of the ship hull as shown in figure 2B by *(X_{exp}, Y_{exp}, Z_{exp})*. In the current study, two sets of bending moment values were computed for the different definitions. Bending moments based on the vectors defined in the experimental tests were obtained and used in the comparison for the time averaged values (transient torque and bending moments were not measured). Propulsor unit's torque and bending moments based on the body frame axes were then obtained and used for force fluctuation analysis with both time averaged and transient values.

The order of the surface panels on pod and strut is arbitrary and the arrangement for the current work is shown in figure 3. The pod and strut surface panel geometry was designed to be stored in two separate input files. This arrangement provided a flexibility to allow a number of multiple-object combinations to be computed. For example, a large pod and number of small struts will assemble an underwater vehicle hull with a number of fins. The counting sequence of corner points of each surface panel must be clockwise to ensure the panel surface normal vector is pointing inside the body. The detailed paneling arrangement for propeller blades, hub, nozzle, rudder and ice blockage, etc. was given in (Liu et al. 2001b).

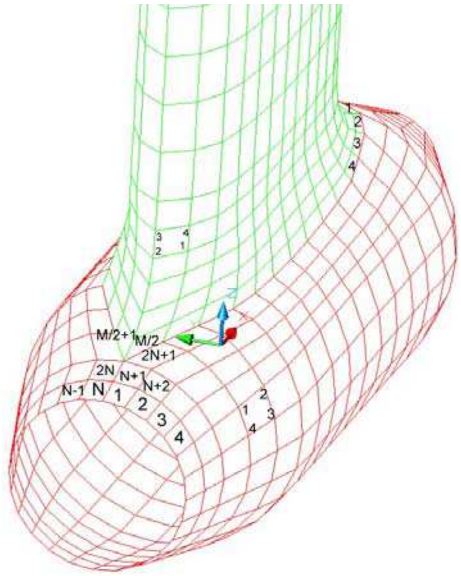

Figure 3. Pod and strut paneling order and corner points counting sequence.

3 RESULTS AND DISCUSSION

In the current work, main concentration was given to obtain the physics of propulsion related forces and unsteady nature of these forces. Prior to running the code to obtain the hydrodynamics of the propulsion performance and unsteady forces, validation and comparison against propulsive performance in previous in-house experiments were made. For various azimuth angles, propulsive performance of a puller type podded propulsor was first validated in terms of propeller shaft thrust and torque coefficients along with thruster coefficient on the pod propulsor unit. Blade bending moment and spindle torque were then obtained and presented. Finally, normal force fluctuations about the propeller shaft and the spindle torque and moments about the pod unit stock were presented. For each category of the results, analysis and discussion were given.

3.1 Code Validation and Comparisons against Measurements

Comparison between the code and previous experimental work was first made for the DTMB P4119 propeller (Jessup 1989 and Gindroz et al. 1998). This is probably the most popular and basic propeller used for marine propeller panel method validation. Figure 5 shows the thrust and torque coefficient comparison for the P4119 propeller in the first quadrant of operation, i.e., from J = 0.0 to $J \approx P/D$. When the advance coefficient J approaches $J \geq P/D$, for most propellers with small or moderate camber sections, thrust becomes diminished.

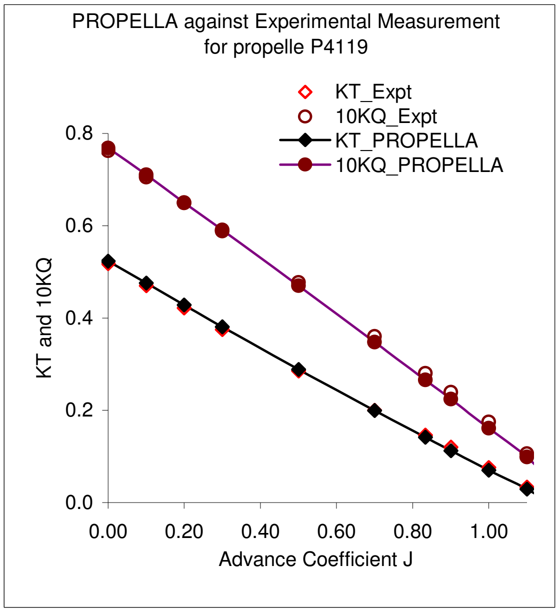

Figure 4. Comparison of propulsive performance of the P4119 propeller between current prediction and previous experimental measurements.

The comparison in figure 4 shows a close agreement between the current code and the previous test results, as the code was tuned up for this propeller. It is also shown that the code well predicts the Kt and Kq curves at both very heavy load condition as well as light ones, consistently.

Further validation and comparison were made for a puller-type bare (no pod or strut) podded propeller with a hub tape angle of 15º. The geometry particulars of the podded propeller under consideration are listed in table 1. This is the base propeller model geometry on podded propeller research program (Liu 2006). The chord distribution was set proportionally the same as the P4119 propeller but the number of blades and expanded area ratio were set differently.

Diameter, D (mm)	270.00
No. of blade	4
Design advance coefficient, J	0.80
Hub-Diameter (h/D) ratio	0.26 (based on regular straight hub)
Angular speed (rps)	15.00
Section thickness form	NACA 66 (DTMB Modified)
Section meanline	NACA = 0.8
Expanded area ratio, EAR	0.60
Pitch distribution	Constant, P/D=1.0
Skew distribution	Zero
Rake distribution	Zero

Table 1. Particulars of the puller-type podded propeller model

Figure 5 show the predicted shaft thrust and torque coefficients of the puller-type podded propeller without pod and strut, comparing with the experimental ones. These experimental results were obtained in-house and were presented previously (Islam et al. to appear).

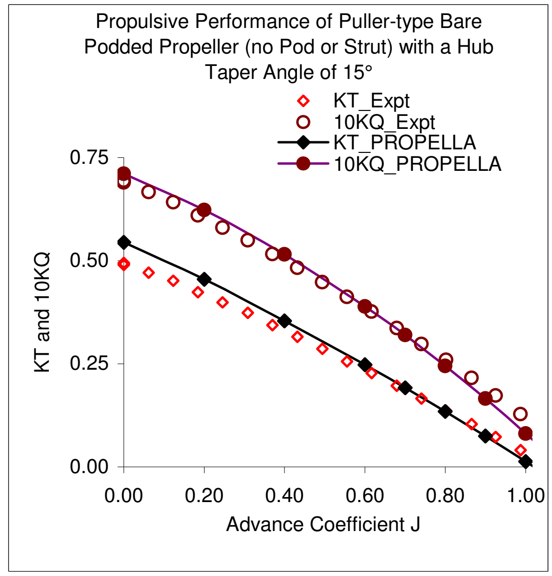

Figure 5. Bare puller-type propeller Kt and 10Kq curves by PROPELLA and measurements

Propeller shaft thrust and torque coefficients, and propulsor unit thrust coefficients for the puller-type 15-degree tape angle propeller with a general pod and strut combination were also predicted by the code PROPELLA and comparison between the code and the in-house experimental tests was carried out. The pod and strut particulars used in the computation are listed in table 2.

Propeller Diameter, D	270 mm
Pod Diameter, D_Pod	139 mm
Pod Length, L_Pod	410 mm
Strut Height, S_Height	300 mm
Strut Chord Length	225 mm
Strut Distance, S_Dist	100 mm
Strut Width	60 mm
Fore Taper Length	85 mm
Fore Taper Angle	15°
Aft Taper Length	110 mm
Aft Taper Angle	25°

Table 2. Geometry particulars of the pod and strut under consideration

The surface mesh paneling of the puller-type propeller-pod-strut assembly generated by the pre- and postprocessor of PROPELLA is shown in figure 6.

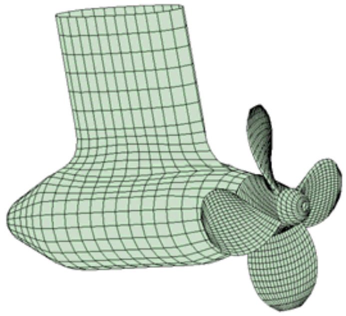

Figure 6. Surface panel mesh of the propeller-pod-strut assembly for the current numerical hydrodynamics tasks.

Figures 7, 8 and 9 show the comparison of propeller shaft thrust and torque coefficients for the puller-podded propeller with an azimuth angle of 0 (straight-ahead), 15 and 30 degrees, respectively.

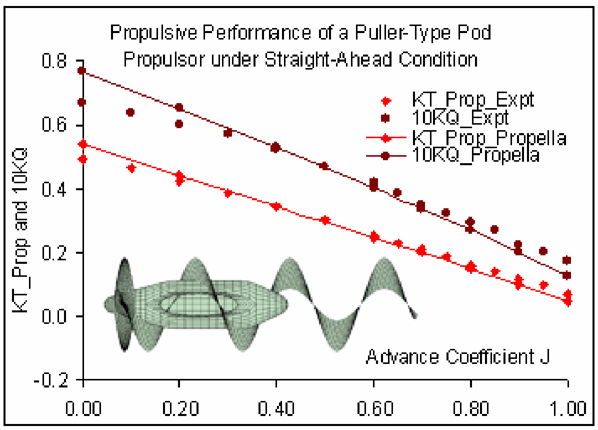

Figure 7. Thrust and torque coefficient comparison for a puller propeller-pod-strut assembly at straight-ahead condition

In figure 7, it shows that the predicted and measured thrust and torque values agreed well, for the whole first quadrant with a little discrepancy at the bollard pull condition and very high speed condition. For simplicity, in the figure, the shed wake vortices for only one blade are shown.

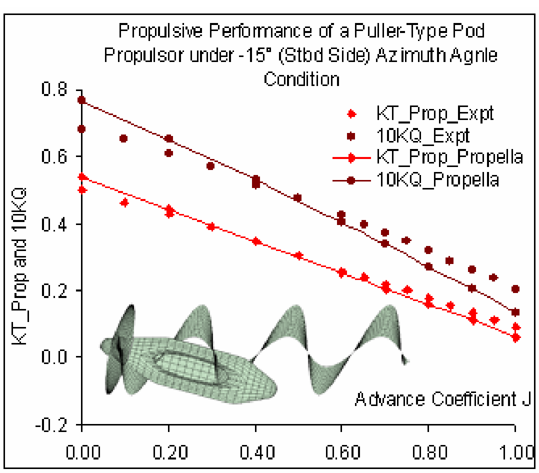

Figure 8. Thrust and torque coefficient comparison for a puller propeller-pod-strut assembly at an azimuth angle of -15 degrees.

In figure 8, it can be seen that while a general agreement in thrust and torque coefficient between the code and the experiment was obtained, with the increase in azimuth angle, the discrepancy became obvious at both bollard pull and very high *J* conditions, where a very high *J* refers to a *J* value approaching the value of pitch-diameter ratio, *p/D*, i.e., at $\frac{J}{p/D} \approx 1.0$. This condition represents an extreme load condition, i.e. the lightest meaningful load conditions for a propeller to produce a positive (forward) thrust in the first quadrant.

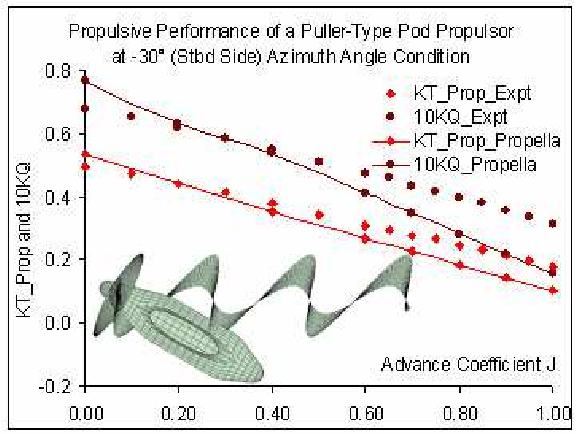

Figure 9. Thrust and torque coefficient comparison for a puller propeller-pod-strut assembly at an azimuth angle of -30 degrees.

In Figure 9, it shows an increasing discrepancy, especially for the shaft torque coefficient at the very lightly loaded condition, between the prediction and the measurements. When azimuth angle becomes large, the propeller and pod-strut interaction becomes dominant, especially due to viscous effect, which needs to be further addressed.

The behavior and the trend in comparison between prediction and measurements for the +15 and +30 azimuth angle cases are similar to the -15 and -30 cases above. They are not shown here.

Figures 10 and 11 show, at a zero azimuth angle, the propeller bearing force (about shaft centre) and the torque and bending moments about the pod unit stock origin P_2 (see figure 2B for reference). In the experimental set-up, point P_2 is located at 0.213 meter (*0.7889D*) downstream and 1.68 meters (*6.222D*) above the origin of the propeller. As in the experimental set-up the distance between the propeller origin and the propulsor unit stock bearing centre is too high to be applicable for shipbuilding consideration, unit stock bearing bending moment about the transverse *y-axis*, *My,* was used for comparison purpose only (see figures 11, 13, and 15 below).

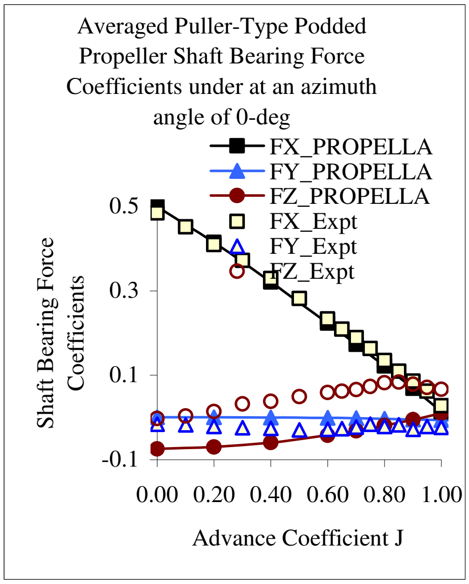

Figure 10. Comparison of time averaged propeller shaft bearing forces between prediction and measurement under zero azimuth angle condition, in the inertia frame.

In figure 10, both the code and the experimental set-up used the same global frame (not body frame). For design consideration, forces presented here based on the global frame need to be transferred to the body frame. It can be seen that the results by the code and the measurements agreed very well, with only some small discrepancy for the vertical force.

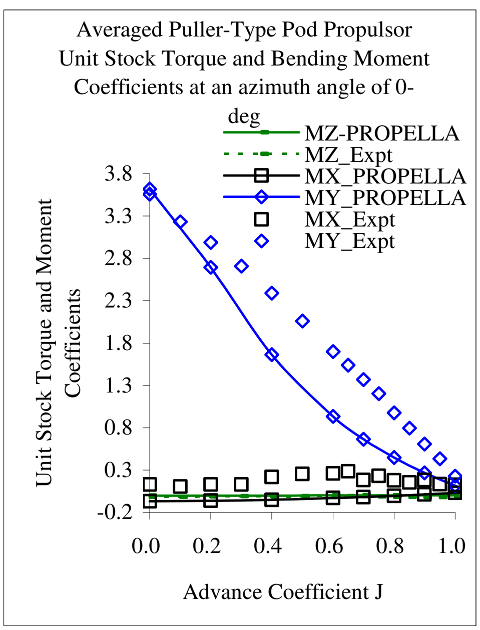

Figure 11. Comparison of time averaged propulsor unit's stock spindle torque, bending moments between prediction and measurement under zero azimuth angle condition.

Again, the predicted and the measured results agreed well, except a minor discrepancy occurred for the bending moment coefficient M_y. The origin of the experimental set-up for the stock bearing location was set at *(0.213, 0.000, 1.680)* in meters relative to the propeller centre or the origin of the body frame defined in the code (see figure 2 for detail). It is also noted that as the stock bearing location was set far away from the body frame origin of *1.68/0.27=6.222D,* more than *6* times of the propeller diameter, the time averaged moment efficient M_y value, mainly contributed by the thrust force, is extremely high. In practice, the averaged sock bearing location should be much lower and the stock torque and moments for a lower stock bearing location of *1.0D* above the origin of the body frame will be presented later.

Figures 12 to 13 and 14 to 15 show the averaged propeller bearing force (about shaft centre) and the torque and bending moments based on the pod unit stock origin point P_2, for the puller propeller-pod-strut assembly at an azimuth angle of *-15* and *-30* degrees, respectively.

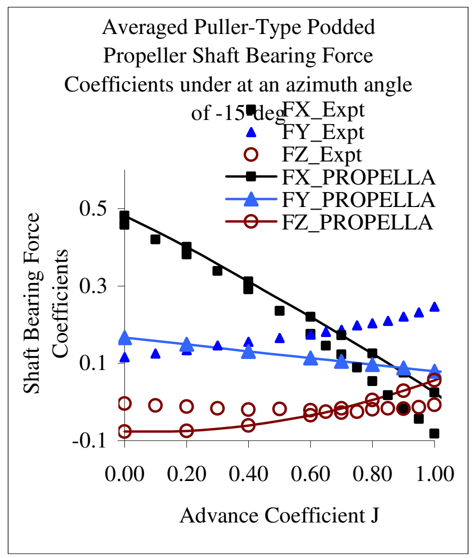

Figure 12. Comparison of time averaged propeller shaft bearing forces between prediction and measurement under *-15*-deg azimuth angle condition.

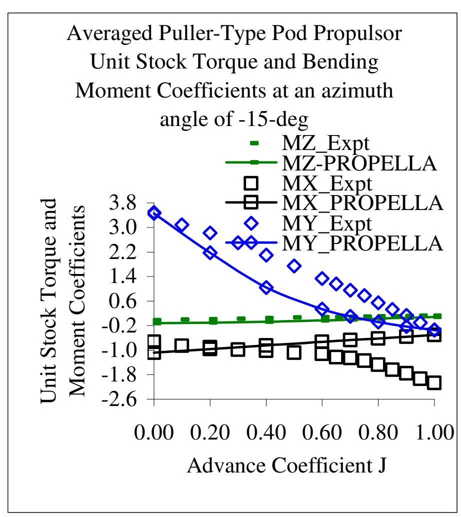

Figure 13. Comparison of time averaged propulsor unit's stock spindle torque, bending moments between

prediction and measurement under -*15*-deg azimuth angle condition.

In figures 12 and 13, an overall agreement between the prediction and the measurements was obtained. Discrepancy became larger at lightly loaded condition at *J* larger than *0.6*. The predicted and the measured shaft thrust force and the propulsor stock unit's spindle torques agreed consistently in the whole first quadrant of operation.

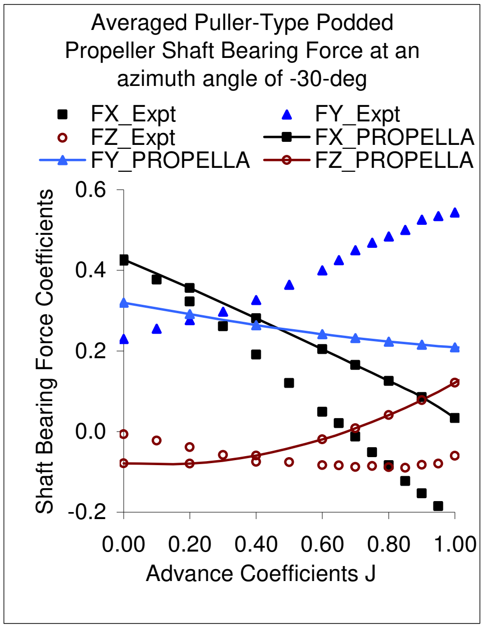

Figure 14. Comparison of time averaged propeller shaft bearing forces between prediction and measurement under -*30*-deg azimuth angle condition.

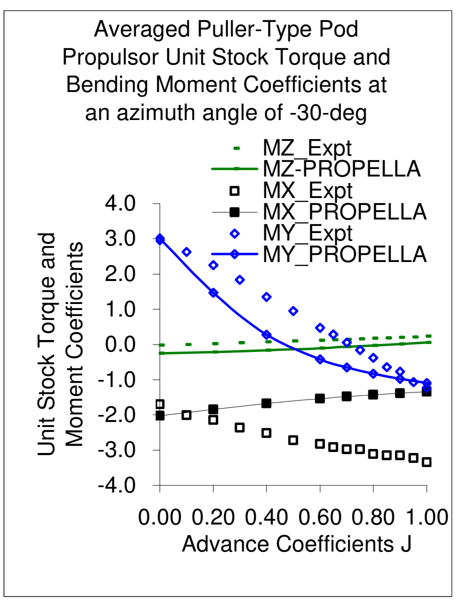

Figure 15. Comparison of time averaged propulsor unit's stock spindle torque, bending moments between prediction and measurement under -*30*-deg azimuth angle condition.

With the increase of the azimuth angle up to a large value at *-30* degrees, discrepancies between prediction and measurement for both propeller shaft normal forces become large, though the discrepancies on the unit stock's torque and bending moment are small except for the M_x bending moment (moment for ship roll motion).

3.2 Unsteady Forces on Shaft，and Unit Stock

In this section, transient forces in time history in terms of fluctuations were obtained and compared with the time averaged ones. These fluctuations were not available from the in-house measurements or in literature. Figures 16 and 18 show the time averaged and transient propeller shaft thrust and torque coefficients at bollard pull condition.

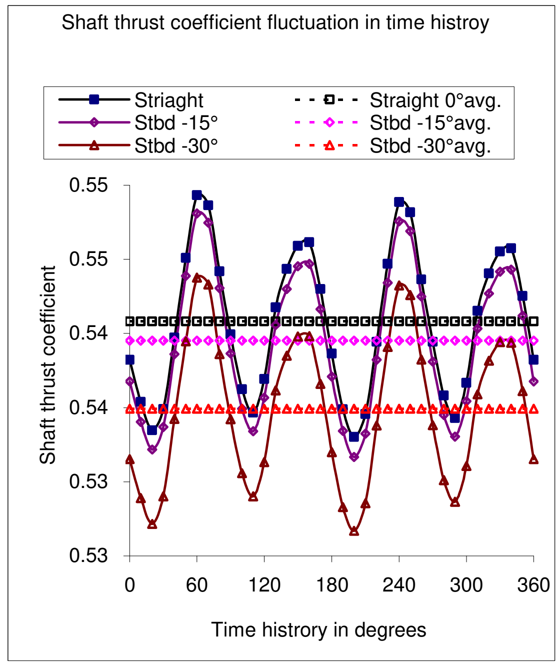

Figure 16. Time averaged and transient thrust force for the puller propeller-pod-strut assembly at various azimuth angles.

In figure 16, as the propulsor is working under zero speed of advance condition, the highest thrust production occurred at a zero azimuth angle, because for all the azimuth angles, speed of advance of both the propulsor unit and the ship was zero at $J=0.0$ and the propeller is working under uniform inflow condition at the zero azimuth angle. The relationship between the advance coefficient of propulsor and the advance coefficient of the ship is defined as $J = J_{ship}\cos(\theta)\cos(\beta)$. With the increase of the J_{ship} value, when the J value of the propulsor is sufficiently smaller than J_{ship}, thrust production acting along the propeller shaft for the larger azimuth angle will become larger. This effect was evidenced from both prediction and measurement but not shown here. The fluctuation of the shaft thrust is about *3%* of the time averaged value which is not significant.

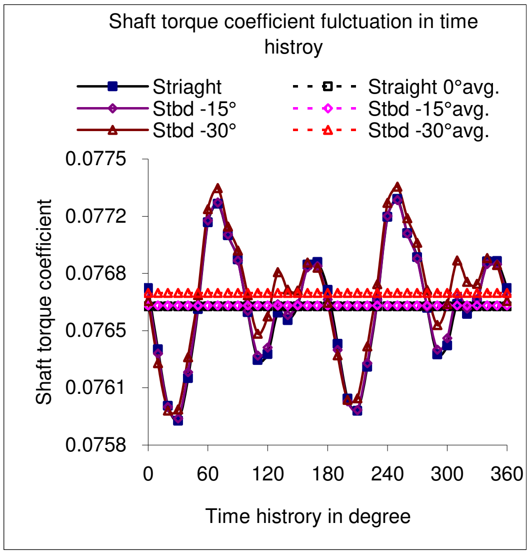

Figure 17. Time averaged and transient shaft torque coefficient for the puller propeller-pod-strut assembly at various azimuth angles.

The same trend as the thrust coefficient fluctuation can be seen for the torque coefficient in figure 17. Cases for positive azimuth angles have a similar trend so they are omitted here.

Figures 18, 19 and 20 show the fluctuation of the bending moment and spindle (steering) toque coefficient for the podded propulsor with a stock bearing location at *(0.213, 0.000, 0.270)* meters, relative to the origin of the body frame. The none-dimensional values of the location are *(0.789D, 0.000D, 1.000D)*.

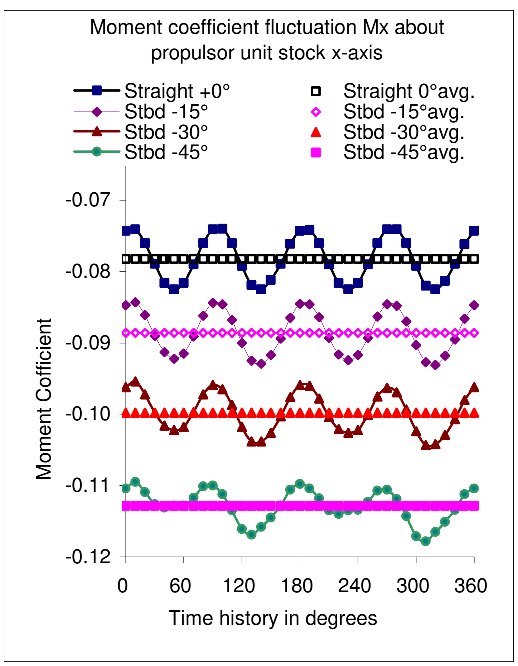

Figure 18. Propulsor unit stock bearing's in-plane bending moment fluctuation at various azimuth angles.

The ship rolling moment fluctuation M_x in figure 18 is small for all azimuth angles. However, the magnitude for a large angle, say, at *45* degrees, is about *150%* of the propeller shaft torque, which is significant with regards to safety in maneuvering operation.

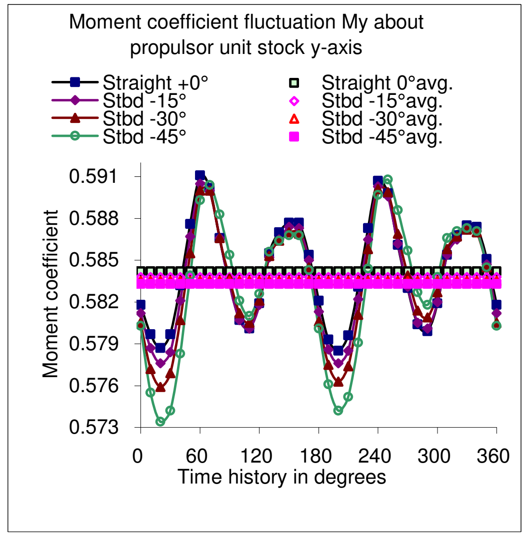

Figure 19. Propulsor unit stock bearing's out-of-plane bending moment fluctuation at various azimuth angles.

Figure 19 shows the ship trim moment coefficient due to the variation of thrust fluctuation. The largest fluctuation occurred for the largest azimuth angle of *45* degrees. The trough-to-peak fluctuation is about *3%* which is little. The magnitude of the trim moment coefficient, however, is about 10 times of the propeller shaft torque, which is similar to a conventional propulsor system.

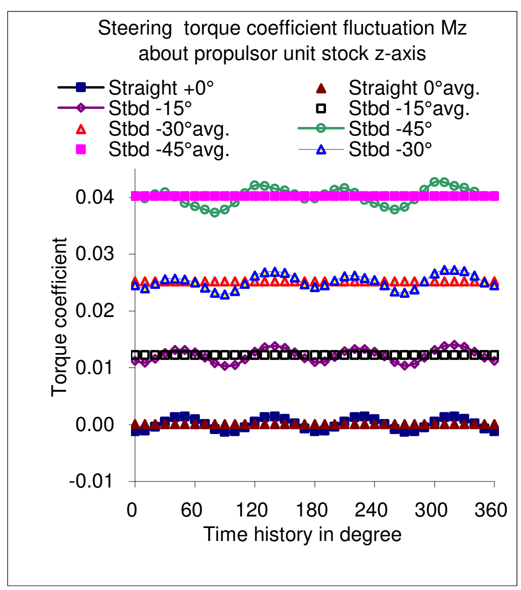

Figure 20. Propulsor unit stock bearing's spindle (steering) torque bending moment fluctuation at various azimuth angles.

Figure 20 shows the steering torque coefficients of the propulsor unit. With an increase of the steering angle (azimuth angle), this torque increased dramatically. Fluctuation in steering torque is also very small (less than *1%*).

It is also noted that the forces and moments referred in this work are hydrodynamic forces only so they do not include the weight of the propulsor unit. When this is included, the vertical force at the unit stock bearing and the ship trim moment mainly due to thrust would be increased as well.

4 CONCLUSIONS

Numerical tool development work was performed and the tool was used to predict the unsteady hydromechanics of the propeller-pod-strut assembly. Validation and comparison were made before the prediction runs. Unsteady fluctuations of the forces, under various constant steering angle, including propeller shaft thrust and torque, steering torque and bending moment at the propulsor unit stock bearing, were obtained and analyzed. It indicates that the most significant magnitude of fluctuation occurred for the blade root section, in terms of blade sectional bending moment and spindle torque. This implies a strong fatigue strength requirement for propeller blade section. Force fluctuations at the propulsor unit stock bearing location are small which indicates that the strength of stock bearing should be based on static forces. However, predicted ship rolling moment at a large azimuth angle of 45 degrees, is about *150%* of the torque on the propeller shaft when the shaft is *1.0D* below the stock bearing. This outstanding value will have a strong effect on maneuvering safety. All the predicted forces and moments above are hydrodynamic loads only. The weight of the propulsor unit was not included. A substantial increase in the vertical force on the stock bearing and a small increase in the ship trim moment are expected when the weigh of the propulsor unit is considered.

Acknowledgement

The authors thank National Research Council Canada, Natural Sciences and Engineering Research Council, Memorial University of Newfoundland, Oceanic Consulting Corporation and Thordon Bearing Ltd for their support. The authors are also grateful for the proofread assistance by Mr. Derek Yetman.

REFERENCES

Gindroz, B., Hoshino, T., & Pylkkanen, J. (editors). (1998). The 22nd ITTC Propulsion Committee Propeller RANS/Panel Method Workshop, Grenoble, France.

He, M., Veitch B., Bose N. & Liu P. (2005). "An Investigation on Wake/Strut Interaction of a Tractor-Type Podded Propulsor". Proceedings of the 7th CMHSC, Halifax, NS Canada.

He, M., Veitch, B., Bose, N., Colbourne, B. & Liu, P. (2007a). "Development of a Three Dimensional Wake Impingement Model and Applications on Oscillating Foils in Tandem". Ocean Engineering, Vol **34/8-9**, pp. 1197-1210.

He, M., Veitch, B., Bose, N., Colbourne, B. & Liu, P. (2007b). "Simulation of Surface Pressure Induced by Vortex/Body Interaction". Journal of Ship Mechanics, Vol. **11**, No. 6, pp. 813-819.

Hess, J.L. & Valarezo, W.O. (1985). "Calculation of steady flow about propellers by means of surface panel method". Proceedings, Research and Technology Douglas Aircraft Company, Long Beach, CA.

Hoshino, T. (1993). "Hydrodynamic Analysis of Propellers in Unsteady Flow Using a Surface Panel Method". Journal of The Society of Naval Architects of Japan, Vol. **174**, pp. 71-87.

Islam, M. F. (2004). "Numerical investigation on effects of hub taper angle and Pod-strut geometry on propulsive performance of pusher Propeller configurations". Master's Thesis, Memorial University of Newfoundland, Canada, 136 p.

Islam M. F, Veitch B, Akinturk A, Bose N & Liu P. (to be submitted). "Performance Study of Podded Propulsor in Static Azimuthing Conditions".

Islam, M.F., Veitch, B., Bose, N. & Liu, P. (2006). "Effects of Hub Taper Angle on the Performance of Podded Propellers". Marine Technology, Vol. **43**, No. 1, pp. 1-10.

Jessup. S. (1989). "An experimental investigation of viscous aspects of propeller blade flow". PhD Thesis, the Catholic University of America, Washington, D.C.

Katz, J. & Plotkin, A. (1991). Low-speed Aerodynamics, McGraw-Hill, New York, 632 p.

Kerwin, Justin E., Kinnas, Spyros A., Lee, Jin-Tae, & Shih, Wei-Zen. (1987). "A Surface Panel Method for the Hydrodynamic Analysis of Ducted Propellers". *Trans. SNAME*, Vol. **95**. pp. 93-122

Liu, P. (1996a). "A Time-domain Panel Method for Oscillating Propulsors with both Chordwise and Spanwise Flexibility". Ph.D. Thesis, Memorial University of Newfoundland, Newfoundland, Canada, 226p.

Liu, P. (1996b). *"Software Development on Propeller Geometry Input Processing and Panel Method Predictions of Propulsive Performance of the R-Class Propeller"*. MMC Engineering & Research Report, No. **1**, NL Canada, 50 p.

Liu, P. (1996-2009). PROPELLA Manual, 50 p.

Liu, P. (2002). "Design and implementation for 3-D unsteady data visualization using object-oriented MFC and OpenGL". CFD Journal of Japan CFD Society, Vol. **11**, no. 3, pp. 335-345.

Liu, P. (2005). "Propulsive performance of a twin-rectangular-foil propulsor in a counter-phase oscillation". Journal of Ship Research (JSR), Vol. **49**, No. 3, pp. 207-214.

Liu, P. (2006). “The Design of a Podded Propeller Base Model Geometry and Prediction of Its Hydrodynamics”. Technical Report, Institute for Ocean Technology, National Research Council Canada (IOT-NRC), Report No.: **TR-2006-16**, 16p.

Liu, P., Akinturk, A., He, M., Islam, M. and Veitch, B.(2008). “Hydrodynamic performance evaluation of an ice class podded propeller under ice interaction”. Proceedings of OMAE 2008, Estoril, Portugal.

Liu, P. & Bose, N. (1997). “Propulsive Performance from Oscillating Propulsors with Spanwise Flexibility”, Proc. R. Soc. Lond. A, Vol. **453**, No. 1963, pp. 1763-1770.

Liu, P. & Bose, N. (1998) "An Unsteady Panel Method for Highly Skewed Propellers in Non-Uniform Inflow". 22nd ITTC Propulsion Committee Propeller RANS/Panel Method Workshop, Grenoble, France, pp.343-349.

Liu, P. & Bose, N. (1999). "Hydrodynamic characteristic of a lunate-shaped oscillating propulsor". Ocean Engr., Vol. **26**, pp.519-529.

Liu, P., Bose, N. & Colbourne, B. (2001a). "Incorporation of a critical pressure scheme into a time-domain panel method for propeller sheet cavitation". International Workshop on Ship Hydrodynamics (IWSH2001), Wuhan, China.

Liu, P., Bose, N. & Colbourne, B. (2001b). "Automated Marine Propeller Geometry Generation of Arbitrary Configurations and A Wake Model for Far Field Momentum Prediction". International Ship Building Progress (ISP), Vol. **48**, Issue 4, pp. 351-381.

Liu, P., Bose N. & Colbourne, B. (2002). "Use of Broyden’s Iteration for an Unsteady Numerical Kutta Condition". International Shipbuilding Progress (ISP), Vol. **49**, no. 4, pp. 263-273.

Liu, P., Islam, M.F., Doucet, M.J., McNeil, A. & Prior, A. (2006). “Design and optimization of an ice class propeller under shallow water, semi-tunnel hull and heavy load conditions”. Proceedings of OMAE 2006, 25th International Conference on Offshore Mechanics and Arctic Engineering, Hamburg, Germany.

Veitch, B., Bose, N., Meade, C. & Liu, P. (1997), “Predictions of Hydrodynamic and Ice Contact Loads on Ice Class Screw Propellers”. Proceedings of the 14th International Conference on Offshore Mechanics and Arctic Engineering (OMAE), Yokohama, 7 p.